Available online at www.sciencedirect.com
ScienceDirect
Tetrahedron
Tetrahedron 63 (2007) 1987–1994

Synthesis and characterization of manganese and copper corrole xanthene complexes as catalysts for water oxidation

Yan Gao,[a] Jianhui Liu,[a,*] Mei Wang,[a] Yong Na,[a] Björn Åkermark[b] and Licheng Sun[a,c,*]

[a]*State Key Laboratory of Fine Chemicals, DUT-KTH-Joint Education and Research Center on Molecular Devices, Dalian University of Technology (DUT), Zhongshan Road 158-40, 116012 Dalian, China*
[b]*Department of Organic Chemistry, Arrhenius Laboratory, Stockholm University, 10691 Stockholm, Sweden*
[c]*Department of Chemistry, Organic Chemistry, Royal Institute of Technology (KTH), 10044 Stockholm, Sweden*

Received 31 August 2006; revised 18 December 2006; accepted 20 December 2006
Available online 22 December 2006

Abstract—Two corrole xanthene ligands and four corresponding Mn^{IV} and Cu^{III} complexes have been synthesized and spectroscopically characterized. This kind of complexes, comprising of xanthene and corrole linked by an amide bond, were designed as bio-inspired models for the oxygen evolving complex (OEC) in Photosystem II. We find that both manganese complexes **4a** and **5a** have efficiency on catalyzing oxygen evolution at low potential (about 0.80 V) by electrochemical method, which is a significant progress in the study of dioxygen formation.

1. Introduction

It has been known that in nature water can be oxidized to evolve O_2 by an oxygen evolving complex (OEC) in Photosystem II (PSII).[1–4] The structure of OEC has been extensively studied by spectroscopic, EPR, crystallographic, and X-ray absorption techniques.[5–8] Although the mechanism of water oxidation has not been clearly determined, it is believed that a high-valent terminal oxo manganese species or the coupling of bridging oxo unit was involved in this process. Numerous experimental and theoretical approaches to this subject have been reported recently and many Mn complexes have been synthesized as artificial OEC models.[9–16] For example, multiporphyrin arrays, dimeric porphyrins with aryl linkages, including those presented in a face to face manner, had been studied extensively.[17–21] The two porphyrin macrocycles in a face to face manner can increase the ability to hold the two metals in a suitable geometry, leading to the possible joint bonding of a dioxygen. Recent studies proved that corroles had advantage to stabilize high-valent metal ions.[22–29] Furthermore, the face-to-face bis-corrole analogues had more advantages in stabilizing high-valent manganese. However, the research for the corrole-based dimeric face-to-face complexes has been studied sparsely. The aryl bridged dimeric corrole was unknown until the first rational synthesis by Guilard in 1998,[30] followed by several reports describing the synthesis and properties of dimeric corroles.[31–35] Up to now, the two corrole subunits in almost all of the bis-corroles reported in the literature were connected to the bridging aryl in a single C–C bond. To design novel potential water oxidation catalysts, we tried to build new models of corrole xanthene, in which the C–C bond linkage would be replaced by an amide group. Such alterations in the structure of models offered more flexibility of the space between the two corrole units to tolerate the different size of the holding parts, hoping for a better geometry for the water oxidation. Since xanthene is a widely used bridge unit, some (bis)-porphyrins or bis-corrole complexes bridged with xanthene have been synthesized.[35–37] It was also found that there was a water molecule combined in the crystal of iron(III)-hydroxide complex Fe–OH(HPX–CO_2H) (HPX=hanging porphyrin xanthene) through a hydrogen bond.[36] This water fixation ability was expected to make xanthene bridged metal corrole a good candidate in the catalytic water oxidation. Thus, xanthene was chosen as a connection unit in our studies. In this paper, we describe the syntheses and properties of the single armed corrole xanthene **4** and double armed corrole xanthene **5** as well as their Mn (**4a** and **5a**) and Cu complexes (**4b** and **5b**). Electrochemical studies of these complexes have been performed. It was found that both complexes **4a** and **5a** were capable of oxidizing water to molecular oxygen electrochemically at low potential in basic solution, and that **5a** had higher catalytic efficiency. This preliminary study will provide the basis for our subsequent mimicking of PS II for water oxidation reaction.

Keywords: Metal corrole complex; Synthesis; Electrochemistry; Oxygen evolution.
* Corresponding authors. Tel.: +86 411 88993886; fax: +86 411 83702185; e-mail addresses: liujh@dlut.edu.cn; lichengs@kth.se

0040–4020/$ - see front matter © 2006 Elsevier Ltd. All rights reserved.
doi:10.1016/j.tet.2006.12.060

2. Results and discussion

2.1. Synthesis and characterization

The synthesis of the new corroles is outlined in Scheme 1. They were obtained in four steps starting from *meso*-triarylcorrole **1**, which was prepared according to a literature method.[38,39] Reduction of the nitro-corrole **1** by $SnCl_2$ in acidic medium afforded the amino analogue **2**. A reaction between the acid chloride **3** and amino-corrole **2** in a ratio of 1:1 and 2:1 gave the desired single armed corrole compound **4** (HCX) and the double armed corrole compound **5** (BCX), respectively. We noticed that the addition order was crucial for this transformation. It was favorable to add the CH_2Cl_2 solution of **2** and TEA to the intermediate **3**, which was freshly prepared by refluxing $SOCl_2$ with xanthenedicarboxylic acid for 2 h. If the addition order was reversed, the yield decreased from ca. 70% to 45% because of the unstable intermediate **3**. Stoichiometric ratio and low temperature were required in order to get a thorough control of the selectivity to allow attachment of just one corrole to the xanthene. The reaction was also influenced by time and temperature. Longer time (>2 h) and higher temperature (>25 °C) led to the decrease of the yield. A subsequent coordination of $Mn(OAc)_2\cdot 4H_2O$ to **4** and **5** furnished complexes **4a** and **5a** in good yields. The Cu corrole complexes were obtained by reaction with $Cu(OAc)_2\cdot H_2O$ in pyridine at room temperature.

Spectroscopic characterization by ^{1}H NMR (for **4**, **5**, **4b**, and **5b**), MS, and UV–vis was used to verify the structures. Although the ^{1}H NMR spectra were difficult to interpret because of the intricate structures, the peaks in the API-MS met with the structures. The peak located at 960.5 corresponds to $[M-H]^-$ (negative mode) for the monomeric corrole **4** and the most intense peak at 1513.8 corresponds to $[M+H]^+$ (positive mode) for the dimeric corrole **5**. The thermal stability of the metal complexes (**4a**, **4b**, **5a**, and **5b**) is greatly improved compared to the free ligands **4** and **5**. In the ^{1}H NMR spectrum of **4b**, signals located at δ 10.11 and 8.23 are attributed to the carboxylic and amide proton, respectively. The ^{1}H NMR spectrum of **5b** is shown in Figure 1. The signal located at δ 8.80 is assigned to the two amide protons. The methyl group of *tert*-butyl, xanthene, and tolyl appears at δ 1.40, 1.56, and 2.29, respectively. In contrast, the paramagnetic property of Mn complexes **4a** and **5a** made it impossible to show well-resolved ^{1}H NMR spectra.

High resolution mass spectrometry (HRMS) was used to further characterize the Mn complexes. The HRMS spectrum of **5a** ($M=C_{103}H_{82}Cl_2Mn_2N_{10}O_3$), obtained on a micromass Q-TOF Micro by TOF MS ES+(positive mode), is shown in Figure 2. The calculated data are 808.7661 $[(M-2Cl)/2]^+$ (a_1), 826.2505 $[(M-Cl+H)/2]^+$ (b_1), and 1652.5021 $[M-Cl]^+$ (c_1), and the measured results are 808.5800 $[(M-2Cl)/2]^+$ (a_2), 826.0650 $[(M-Cl+H)/2]^+$

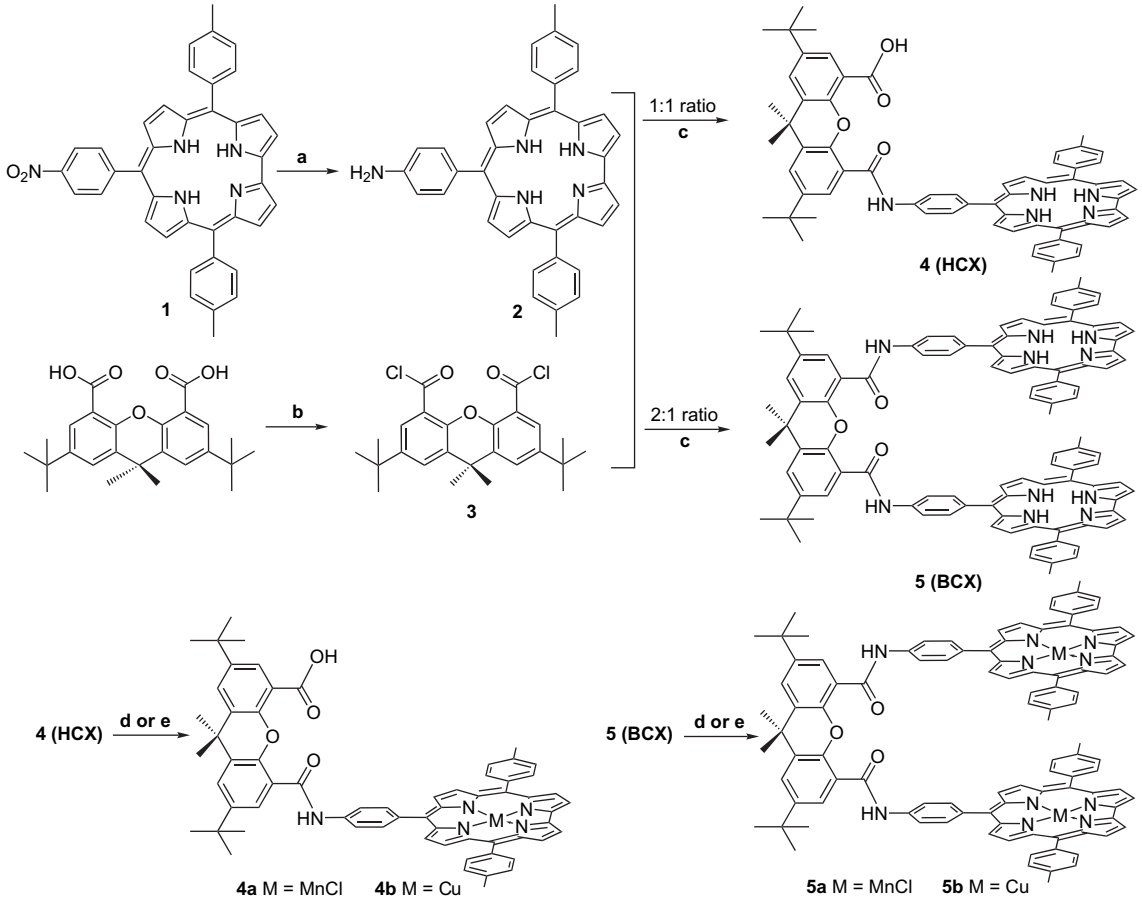

Scheme 1. (a) HCl/AcOH, $SnCl_2\cdot 2H_2O$, $CHCl_3$, 65–70 °C, over night; (b) $SOCl_2$, reflux, 2 h; (c) Et_3N, CH_2Cl_2, rt, 2 h; (d) $Mn(OAc)_2\cdot 4H_2O$, DMF, reflux, 10 min; (e) $Cu(OAc)_2\cdot H_2O$, pyridine, rt, 1 h.

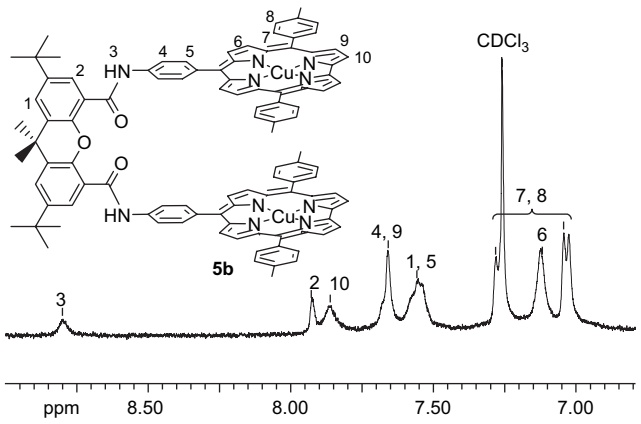

Figure 1. The ^{1}H NMR spectrum of **5b** in $CDCl_3$ at 25 °C.

(b_2), and 1652.5498 $[M-Cl]^+$ (c_2). Through isotope analysis, we find that the measured data match well with the calculated values. By comparing the measured and calculated results, the manganese of complex **5a** can be confirmed to be Mn^{IV}. We characterized the Mn complex **4a** in a similar way.

2.2. UV–vis spectral characterizations

The electronic absorption spectra of two corrole ligands and their metal complexes were recorded in CH_2Cl_2 (**4**, **4a**, and **4b** in Fig. 3a and **5**, **5a**, and **5b** in Fig. 3b). Corrole **4** and its Cu complex **4b** have a similar Soret band at 418 and 419 nm, respectively, while the Soret band of **4a** is located at 437 nm, showing a red shift of 19 nm relative to that of ligand **4**. In the region of the Q-band, ligand **4** shows three well-defined visible bands at 575, 622, and 652 nm, while the Q-bands of **4a** and **4b** are smoother. Complex **4b** has two visible bands located at 545 and 634 nm in CH_2Cl_2 and **4a** has a weak band at ca. 525 nm. The Soret band and Q-band of **4a** are clearly affected by the central Mn ion with an obvious red shift of the Soret band and a blue shift of the Q-band. The behavior of the bis-corrole ligand **5**, its Mn complex **5a** and Cu complex **5b** is similar to those of **4**, **4a**, and **4b**. The valent state of the metal center of the manganese complexes, Mn^{IV}, was confirmed by the characteristic UV–vis spectra.[40,41]

2.3. Electrochemistry

The free-base corroles **4** and **5** could not be measured by cyclic voltammetry (CV) due to their electrochemical lability in solution. The redox potentials of the manganese (**4a** and **5a**) and copper complexes (**4b** and **5b**) were measured by CV in CH_2Cl_2 containing 0.1 M $TBAPF_6$ (Fig. 4) and the data are collected in Table 1. Complex **4a** undergoes a single reversible one-electron reduction (Mn^{III}/Mn^{IV}) at $E_{1/2}=-0.32$ V and single reversible one-electron oxidation at $E_{1/2}=0.61$ V (Fig. 4a). Complex **5a** undergoes a single, metal-centered reversible reduction (Mn^{III}/Mn^{IV}) at $E_{1/2}=-0.33$ V and two reversible oxidations at $E_{1/2}=0.58$ and

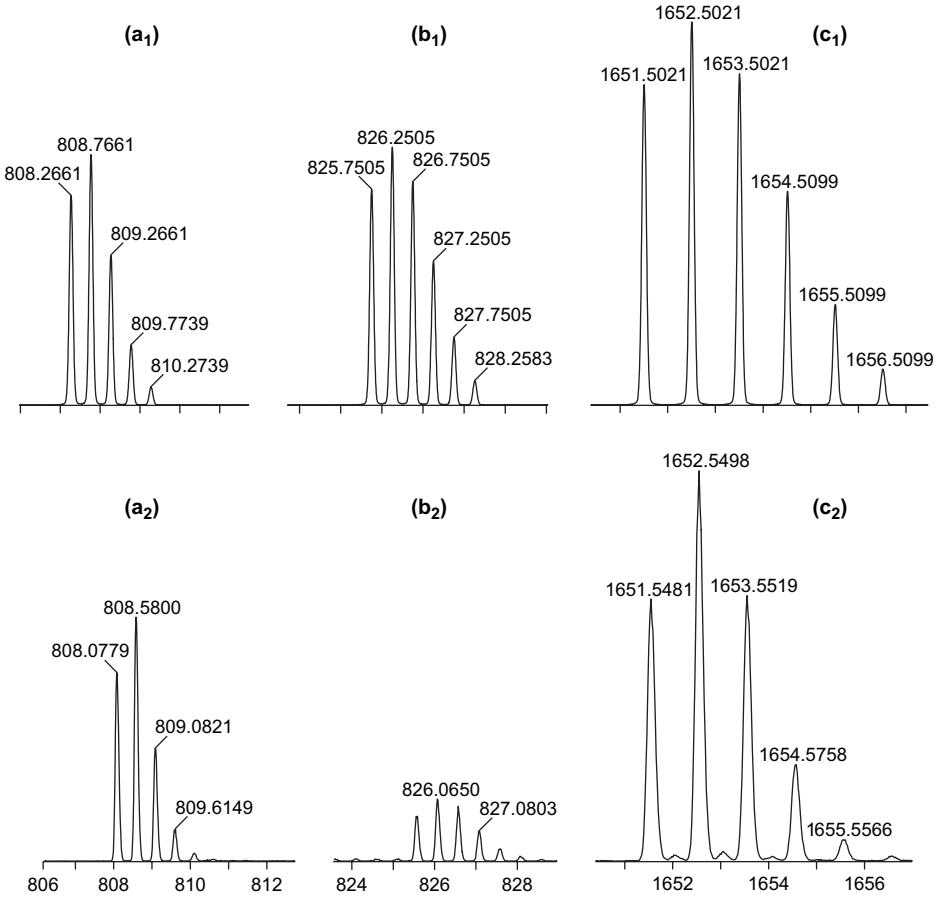

Figure 2. The HRMS of isotope peaks of **5a**. Calculated (top three) $[(M-2Cl)/2]^+$ (a_1), $[(M-Cl+H)/2]^+$ (b_1), and $[M-Cl]^+$ (c_1); Measured (bottom three) $[(M-2Cl)/2]^+$ (a_2), $[(M-Cl+H)/2]^+$ (b_2), and $[M-Cl]^+$ (c_2).

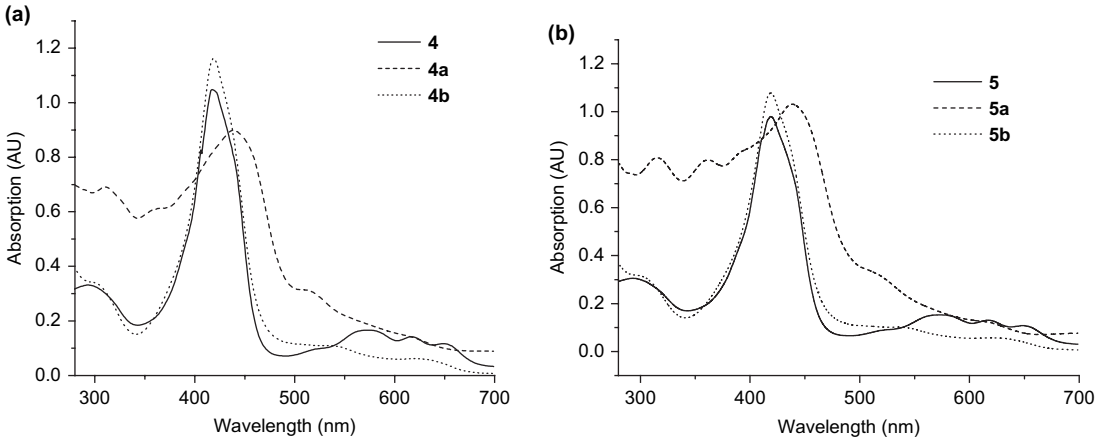

Figure 3. The UV–vis spectra: (a) **4**, **4a**, and **4b** in CH_2Cl_2 and (b) **5**, **5a**, and **5b** in CH_2Cl_2.

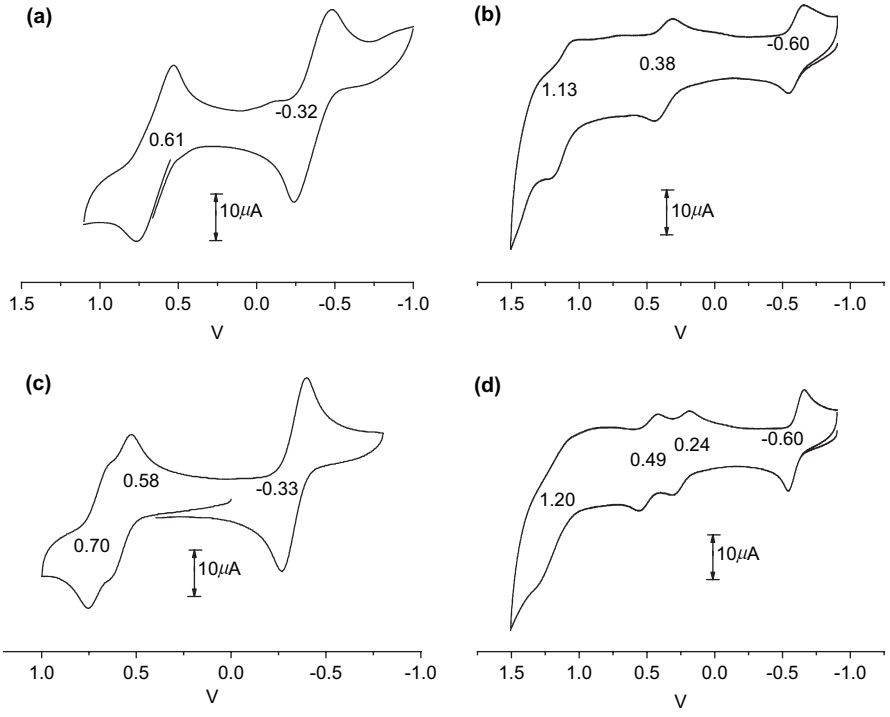

Figure 4. Cyclic voltammetry of **4a** (a), **4b** (b), **5a** (c), and **5b** (d) in CH_2Cl_2: 0.1 M $TBAPF_6$ as supporting electrolyte. Glass carbon as working electrode, $Ag/AgNO_3$ as reference electrode, scan rate=0.1 V/s.

0.70 V (Fig. 4c). The peak currents of the two oxidations are both lower than that of the reduction. The reduction occurred in a one step two-electron process while the oxidation occurred via two one-electron step with the potential difference of 120 mV. The oxidation potential of **4a** was intermediate between the two oxidation potentials of **5a**, while the reduction potentials of the two complexes were essentially identical. This result clearly indicates that there exists a weak interaction between the two Mn corrole subunits in **5a**. The CVs of the manganese complexes **4a** and **5a** are similar to those of the Mn^{IV}[T(*p*-X–P)C]Cl complexes (X=CH_3, H, and CF_3),[40,41] so the oxidation potentials are assigned according to the works of Ghosh[40,41] and Gross,[42] and it is proposed that the oxidations of the Mn^{IV} complexes are corrole-centered oxidation. The reduction processes were assigned by controlled potential UV–vis spectroelectrochemistry.

Table 1. Redox potential data of metal corrole complexes

Compounds	$E_{1/2}$/V versus Ag/Ag^+	
	Reduction	Oxidation
4a	−0.32	0.61
4b	−0.60	0.38, 1.13
5a	−0.33	0.58, 0.70
5b	−0.60	0.24, 0.49, 1.20

$E_{1/2}=(E_{pa}-E_{pc})/2$, $Ag/AgNO_3$ as ref, scan rate=0.1 V/s.

Controlled potential UV–vis spectroelectrochemistry at −0.5 V was carried out for further confirmation of the Mn valent states of **5a**. The corresponding spectral changes are illustrated in Figure 5. The Soret band at 437 nm decreased, while the peaks at 487 and 652 nm increased. This result is consistent with the literature,[29] and in support of the

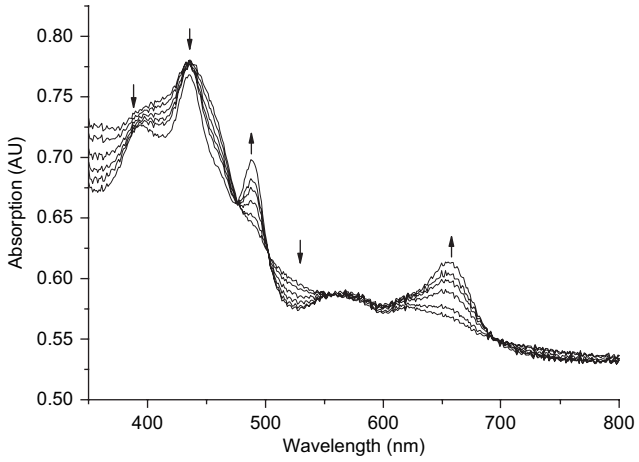

Figure 5. Spectroelectrochemical reduction of **5a** at −0.5 V.

conclusion that the reductions of the complexes are metal-centered (Mn^{III}/Mn^{IV}).

In the similar manner, copper corrole complex **4b** displays three reversible redox processes at $E_{1/2}$=−0.60, 0.38, and 1.13 V. The single reversible one-electron reduction is metal-centered (Cu^{II}/Cu^{III}) and the first oxidation can be assigned to be corrole-centered (Fig. 4b). The redox processes of bis-corrole copper complex **5b** are similar to those of (BCA)Cu_2 (bis-corrole anthracene dicopper),[35] exhibiting a single two-electron reduction of Cu^{II}/Cu^{III} at $E_{1/2}$=−0.60 V, three reversible one-electron oxidation waves at $E_{1/2}$=0.24, 0.49, and 1.20 V (Fig. 4d). The first two oxidations can be safely assigned to a stepwise abstraction of one electron from each corrole macrocycle[35] and the potential separation between the first two oxidations of **5b** is 250 mV, which is 120 mV more than that of (BCA)Cu_2. This result can be attributed to the greater π–π interaction between the two corrole macrocycles in the copper corroles with xanthene spacers. The first oxidation potential of **4b** is also between the first two oxidations of **5b**, as observed for the manganese corroles **4a** and **5a**.

The low oxidation potential of Mn^{III}/Mn^{IV} in complexes **4a** and **5a** indicated that they can be relatively easily oxidized to high-valent manganese complexes. Thus, it seemed interesting to carry out experiments in aqueous medium to examine the possibility of electrochemically catalyzed water oxidation to evolve O_2 in the presence of **4a** and **5a**.

2.4. Electrochemically catalyzed water oxidation

The catalytic activities of complexes **4a** and **5a** in electrochemical water oxidation were evaluated by CV. Multiple scan measurements were performed after addition of *n*-BuNOH (10% in water, 30 μL) to CH_2Cl_2/CH_3CN (2:3, v/v, 5 mL) solution of manganese complex **4a** with potentials ranging from 1.00 to −1.50 V. Before we started the scan, oxygen was eliminated by continuous bubbling of argon. During the first scan cycle, the oxidation occurred at 0.79 V (peak potential E_{pa}) and the reduction process was detected at the potential −1.29 V (full line in Fig. 6, left). When the scan was carried out up to the third and the fourth cycle, the oxidation potential at 0.79 V was unchanged, but the peak at potential −1.29 V was slightly increased (dashed and dotted lines). When we scanned at potentials ranging from 0.50 to −1.50 V, the peak at −1.29 V could not be observed even after several scan cycles. This indicates that the electrochemical reduction process represented by the peak at −1.29 V cannot take place in this system when the scan potential is lower than 0.79 V.

In the same manner, the electrochemical behavior of complex **5a** in basic aqueous solution was recorded by CV (Fig. 6, right). An oxidation peak at 0.80 V (E_{pa}) is observed, but no reduction can be observed at −1.29 V (full line). When the scan was carried out up to the fourth cycle, a peak at −1.29 V appeared and increased distinctly (dashed line). To assign the event at −1.29 V, argon and oxygen were successively bubbled into the solution. When oxygen was added, there was an increase in current intensity of the reduction at −1.29 V (dotted line). This confirms that the reduction peak at −1.29 V is due to the reduction of O_2. Control experiments have been performed. When no Mn complex **4a** or **5a** was added to the solution, no peak increase at −1.29 V was found. The two oxidation potentials for oxygen evolution catalyzed by **4a** (E_{pa}=0.79 V) and **5a** (E_{pa}=0.80 V) are much lower than that reported for porphyrin dimers,[17] which need at least 1.20 V versus Ag/Ag^+ under basic conditions. In contrast, no oxygen formation could be detected by CV when the copper complexes **4b** and **5b** were used.

The oxygen evolution from catalytic water oxidation has been further confirmed by direct detection of oxygen with oxygen electrode unit. The experimental setup consists of

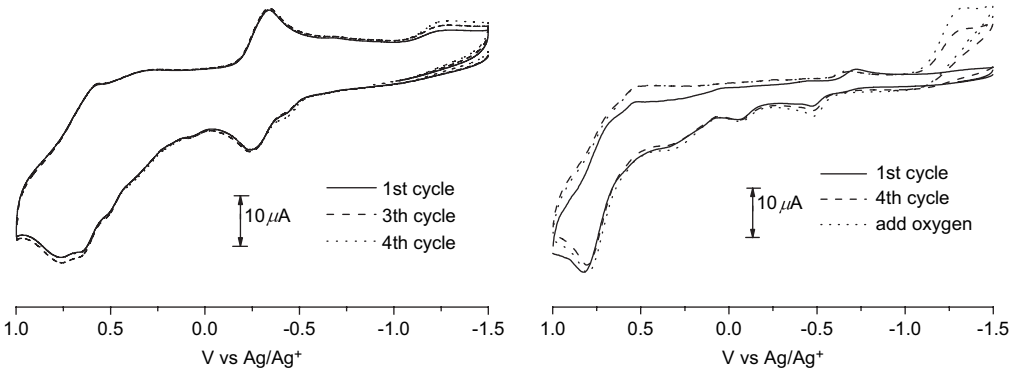

Figure 6. Cyclic voltammograms of **4a** (left) and **5a** (right) in CH_2Cl_2/CH_3CN (2:3) with 30 μL 10% *n*-Bu_4NOH water solution. Reference electrode $Ag/AgNO_3$, electrolyte 0.1 M $TBAPF_6$, scan rate 0.1 V/s.

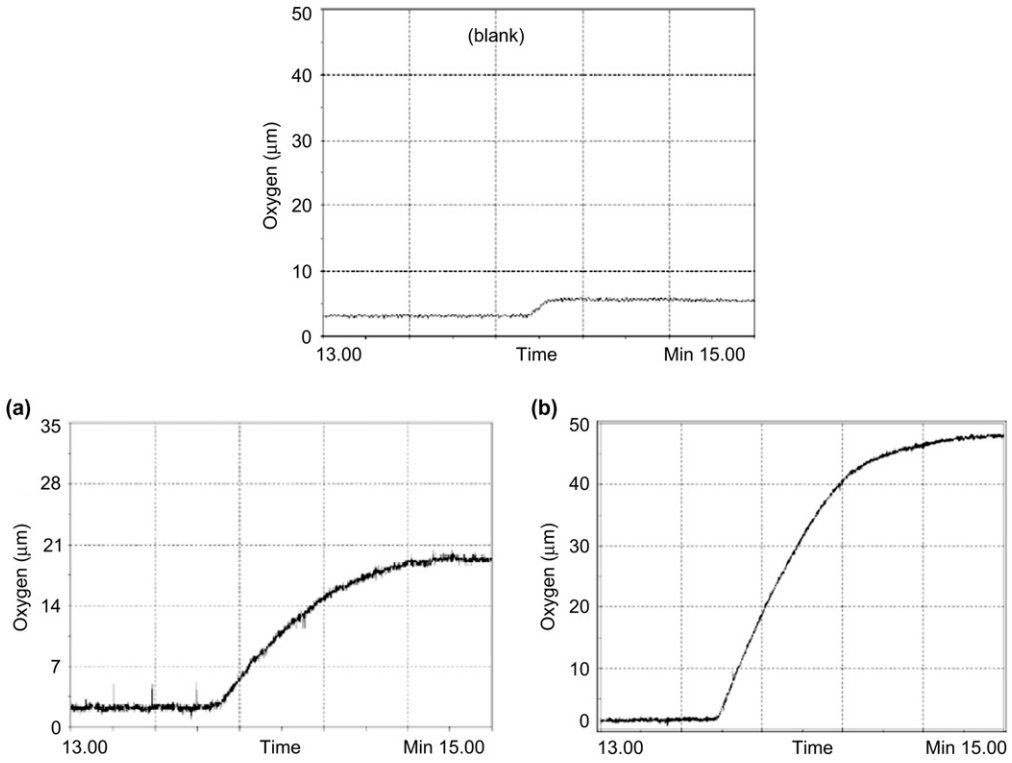

Figure 7. Oxygen evolution versus time for blank, **4a** (a) and **5a** (b).

an airtight electrochemistry cell for catalyzing water oxidation and one oxygen electrode unit for detecting O_2. In a typical procedure, CH_2Cl_2/CH_3CN (2:3, 5 mL), $TBAPF_6$ (90 mg), **4a** (6 mg, 5 μmol), and 30 μL Bu_4NOH (10%) water solution were added into electrochemistry cell, and deionized water was added into oxygen electrode units. Argon was bubbled to the solution to remove O_2 and the oxygen electrode was calibrated to establish a correction curve. After the solution in the electrochemistry cell was electrolyzed at 0.85 V for ca. 13 min at 20 °C, the O_2 generated was carried to the oxygen electrode unit by slowly bubbling argon. The curve (Fig. 7a) proves that the concentration of O_2 in the deionized water increases only from ca. 3.00 μM to 19.20 μM within 1.5 min. The catalytic activity of **5a** was also examined in the same manner. We observed that the curve increased rapidly from 1.50 μM to 47.50 μM within 1.5 min (Fig. 7b). The experiment was also performed in the absence of manganese complexes, and it was observed that the concentration of O_2 increases only from about ca. 3.00 μM to 6.00 μM, which was assigned to the air leakage from the reference electrode. The results show that manganese complexes **4a** and **5a** did function as catalysts for oxygen evolution under basic condition. The catalyst **5a** is almost three times as efficient as **4a**. The investigations of the mechanism of O–O bond formation catalyzed by the Mn complexes **4a** and **5a** are in progress.

3. Conclusion

In conclusion, two corrole ligands **4** and **5** and four metal corrole complexes **4a**, **4b**, **5a**, and **5b** were synthesized and their structures were determined by spectroscopic analyses. They were also electrochemically studied by CV. The electrochemical results indicated that the manganese complexes could be easily oxidized to high-valent states, which might be required for water oxidation. Electrochemical studies show that Mn corrole complexes **4a** and **5a** can catalyze oxidation of hydroxide and possibly also water to produce oxygen at quite low oxidation potentials. It is worth noting that the face-to-face bis-corrole dimeric Mn complex **5a** is a promising catalyst for efficient electrochemical generation of O_2 from water under basic conditions.

4. Experimental

4.1. General

Reagents and instruments: all solvents were dried and distilled prior to use according to the standard methods. Commercially available chemicals were used without further purification. The reagent 2,7-di-*tert*-butyl-9,9-dimethyl-4,5-xanthenedicarboxylic acid was purchased from Aldrich. Proton spectra were collected on a Varian INOVA 400NMR spectrometer. Mass spectra were recorded on an HP1100 MSD instrument. Elemental analyses were performed on a CARLO ERBAMOD-1106 elemental analyzer. The melting points for all new compounds are above 250 °C.

4.1.1. 5,15-Bis-(4-methylphenyl)-10-(4-aminophenyl)corrole (2). To a solution of 5,15-bis-(4-methylphenyl)-10-(4-nitrophenyl)corrole **1** (240 mg, 0.400 mmol) in 1:2 $CHCl_3$/AcOH (30 mL) was added a solution of $SnCl_2 \cdot 2H_2O$ (366 mg, 1.62 mmol) in concentrated HCl (20 mL). The mixture was vigorously stirred in a preheated oil bath (65–70 °C) for 30 min, refluxed over night, and then neutralized with ammonia solution (25%) to pH=8–9. Chloroform

(100 mL) was added, and the mixture was stirred for 1 h. The green organic phase was separated, and the water phase was extracted with $CHCl_3$ (2×100 mL). The combined organic layers were washed once with dilute ammonia solution, three times with water, and then concentrated to dryness. The residue was purified by column chromatography (silica gel and chloroform) to afford pure corrole **2** (150 mg, 67%) as a blue-green solid. API-MS *m/z* 570.2 $[M+H]^+$; UV–vis (CH_2Cl_2) λ_{max} [nm]=289, 412, 523, 566, 619, 650; ^1H NMR (400 MHz, $CDCl_3$, 25 °C) δ 2.68 (s, 6H), 3.99 (br, 2H), 7.06 (br, 2H), 7.62 (br, 4H), 7.95 (br, 2H), 8.25 (br, 4H), 8.56 (br, 4H), 8.87 (br, 4H). Anal. Calcd for $C_{39}H_{31}N_5$: C, 82.22; H, 5.48; N, 12.29. Found: C, 82.22; H, 5.09; N, 12.03.

4.1.2. 2,7-Di-*tert*-butyl-9,9-dimethyl-4-[5,15-bis-(4-methylphenyl)corrol-10-(*N*-4-phenylamido-acyl)]-5-xanthenecarboxylic acid (4). A mixture of 2,7-di-*tert*-butyl-9,9-dimethyl-4,5-xanthenedicarboxylic acid (41 mg, 0.10 mmol) and $SOCl_2$ (5 mL) was refluxed for 2 h. After removing excess of $SOCl_2$ by distillation under reduced pressure, the xanthene acyl chlorine **3** was dried in vacuum at 70 °C for 30 min. Then dry CH_2Cl_2 (5 mL) was added and the mixture was stirred for 5 min at room temperature. A mixture of corrole **2** (57 mg, 0.10 mmol) in CH_2Cl_2 (15 mL) and 2 drops of Et_3N was added dropwise to the resulting light yellow solution (white smoke was observed in the reaction flask). The mixture was stirred for 2 h at 0 °C. It was purified directly by column chromatography on silica gel with a mixture of MeOH/CH_2Cl_2 (1:100) as an eluent to give the desired single armed corrole **4** (65 mg, 68%) as a dark-green solid. API-MS *m/z* 960.5 $[M-H]^-$; UV–vis (CH_2Cl_2) λ_{max} [nm]=343, 418, 575, 622, 652; ^1H NMR (400 MHz, $CDCl_3$, 25 °C) δ 1.43 (s, 18H), 1.72 (s, 6H), 2.65 (s, 6H), 6.98 (s, 1H), 7.38–7.65 (m, 4H), 7.68–7.81 (m, 4H), 7.90–8.13 (m, 4H), 8.17 (br, 4H), 8.54 (br, 4H), 8.70 (br, 2H), 8.89 (br, 2H), 10.62 (s, 1H).

4.1.3. 2,7-Di-*tert*-butyl-9,9-dimethyl-4,5-bis-[5,15-bis-(4-methylphenyl)corrol-10-(*N*-4-phenyl-acyl)]xanthene diamide (5). This compound was prepared in a same manner as **4** from 2,7-di-*tert*-butyl-9,9-dimethyl-4,5-xanthenedicarboxylic acid (40 mg, 0.10 mmol) and corrole **2** (0.12 g, 0.21 mmol) at room temperature and was purified directly by column chromatography on silica gel with a mixture of MeOH/CH_2Cl_2 (1:100) as an eluent to give the desired bis-corrole **5** (105 mg, 70%) as a dark-green solid. API-MS *m/z* 1513.8 $[M+H]^+$; UV–vis (CH_2Cl_2) λ_{max} [nm]=285, 420, 537, 621; ^1H NMR (400 MHz, $CDCl_3$, 25 °C) δ −3.10 (br, 4H), −2.27 (br, 2H), 1.49 (s, 18H), 1.85 (s, 6H), 2.35 (s, 12H), 6.86 (d, 8H, *J*=8.0 Hz), 7.00 (d, 8H, *J*=8.0 Hz), 7.75 (s, 8H), 7.98 (br, 4H), 8.14 (s, 4H), 8.16 (d, 4H, *J*=5.6 Hz), 8.25 (s, 4H), 8.68 (s, 4H), 9.29 (s, 2H).

4.1.4. 2,7-Di-*tert*-butyl-9,9-dimethyl-4-[manganese-5,15-bis-(4-methylphenyl)corrol-10-(*N*-4-phenylamido-acyl)]-5-xanthenecarboxylic acid (4a). A solution of xanthene–NHCO–corrole **4** (100 mg, 0.105 mmol) and excess of manganese(II) acetate tetrahydrate (0.245 g, 1.0 mmol) in DMF (10 mL) was heated to reflux for 10 min. The solvent was evaporated and the residue was dissolved in CH_2Cl_2. It was washed with brine and concentrated to dryness. The residue was purified by column chromatography on silica gel with a mixture of acetone/CH_2Cl_2 (1:100) as an eluent to give **4a** (95 mg, 94%) as a brown solid. API-MS *m/z* 1013.4 $[M-Cl]^+$, 1047.3 $[M-H]^-$; UV–vis (CH_2Cl_2) λ_{max} [nm]=310, 437, 659. Anal. Calcd for $C_{64}H_{56}ClMnN_5O_4$: C, 73.24; H, 5.38; N, 6.67. Found: C, 73.06; H, 5.20; N, 6.51.

4.1.5. 2,7-Di-*tert*-butyl-9,9-dimethyl-4-[copper-5,15-bis-(4-methylphenyl)corrol-10-(*N*-4-phenylamido-acyl)]-5-xanthenecarboxylic acid (4b). A solution of xanthene–NHCO–corrole **4** (96 mg, 0.10 mmol) and excess of cupric acetate (100 mg, 0.5 mmol) in pyridine (5 mL) was mixed and stirred for 1 h. Evaporation of the solvent and column chromatography on silica gel with CH_2Cl_2 as an eluent gave **4b** (90 mg, 88%) as a red-brown solid. API-MS *m/z* 1020.2 $[M-H]^-$, 1056.2 $[M+Cl]^-$; UV–vis (CH_2Cl_2) λ_{max} [nm]=304, 419, 545, 634; ^1H NMR (400 MHz, $CDCl_3$, 25 °C) δ 1.36 (s, 9H), 1.39 (s, 9H), 1.7 (s, 6H), 2.44 (s, 6H), 7.29 (d, 4H, *J*=7.2 Hz), 7.41 (br, 4H), 7.63 (s, 2H), 7.71 (d, 4H, *J*=7.2 Hz), 7.73 (br, 4H), 7.84–7.93 (m, 4H), 8.02 (s, 2H), 8.23 (s, 1H), 10.11 (s, 1H). Anal. Calcd for $C_{64}H_{56}CuN_5O_4$: C, 75.16; H, 5.52; N, 6.85. Found: C, 74.89; H, 5.43; N, 6.77.

4.1.6. 2,7-Di-*tert*-butyl-9,9-dimethyl-4,5-bis-[manganese-5,15-bis-(4-methylphenyl)corrol-10-(*N*-4-phenyl-acyl)]-xanthene diamide (5a). A DMF solution (10 mL) of xanthene–NHCO–bis-corrole **5** (0.15 g, 0.10 mmol) and manganese(II) acetate tetrahydrate (0.49 g, 2.0 mmol) was heated to reflux for 10 min. The solvent was evaporated and the residue was dissolved in CH_2Cl_2. This solution was washed with brine and then concentrated to dryness. The residue was purified by column chromatography on silica gel with a mixture of MeOH/CH_2Cl_2 (1:100) as an eluent to give **5a** (150 mg, 93%) as a brown solid. API-MS *m/z* 808.7 $[(M-2Cl)/2]^+$, 1652.4 $[M-Cl]^+$; UV–vis (CH_2Cl_2) λ_{max} [nm]= 314, 362, 437, 658. Anal. Calcd for $C_{103}H_{82}Cl_2Mn_2N_{10}O_3$: C, 73.26; H, 4.89; N, 8.29. Found: C, 73.12; H, 5.08; N, 7.83.

4.1.7. 2,7-Di-*tert*-butyl-9,9-dimethyl-4,5-bis-[copper-5,15-bis-(4-methylphenyl)corrol-10-(*N*-4-phenyl-acyl)]-xanthene diamide (5b). A solution of xanthene–NHCO–bis-corrole **5** (75 mg, 0.05 mmol) and excess of cupric acetate (100 mg, 0.5 mmol) in pyridine (5 mL) was mixed and stirred for 1 h. Evaporation of the solvent and column chromatography on silica gel with CH_2Cl_2 as an eluent gave **5b** (70 mg, 86%) as a red-brown solid. API-MS *m/z* 1634.8 $[M+H]^+$; UV–vis (CH_2Cl_2) λ_{max} [nm]=419, 545, 634; ^1H NMR (400 MHz, $CDCl_3$, 25 °C) δ 1.40 (s, 18H), 1.56 (s, 6H), 2.29 (s, 12H), 7.04 (d, 8H, *J*=7.2 Hz), 7.12 (br, 8H), 7.28 (d, 8H, *J*=7.2 Hz), 7.51–7.58 (m, 6H), 7.66 (br, 8H), 7.87 (br, 4H), 7.92 (s, 2H), 8.80 (s, 2H). Anal. Calcd for $C_{103}H_{82}Cu_2N_{10}O_3$: C, 75.67; H, 5.06; N, 8.57. Found: C, 75.24; H, 5.22; N, 8.32.

Acknowledgements

Financial support of this work from the following sources is gratefully acknowledged: Natural Science Foundation of China (Grant Nos. 20471013, 20633020, and 20672017), the Ministry of Science and Technology (MOST) (Grant No. 2001CCA02500), the Swedish Energy Agency (STEM), K & A Wallenberg Foundation and The Swedish Research Council (VR).

References and notes

1. Rüttinger, W.; Dismukes, G. C. *Chem. Rev.* **1997**, *97*, 1.
2. Manchanda, R.; Brudvig, G. W.; Crabtree, R. H. *Coord. Chem. Rev.* **1995**, *144*, 1.
3. Pecoraro, V. L.; Baldwin, M. J.; Gelasco, A. *Chem. Rev.* **1994**, *94*, 807.
4. Yagi, M.; Kaneko, M. *Chem. Rev.* **2001**, *101*, 21.
5. Zouni, A.; Witt, H. T.; Kern, J.; Fromme, P.; Krab, N.; Saenger, W.; Orth, P. *Nature* **2001**, *409*, 739.
6. Kamiya, N.; Shen, J. R. *Proc. Natl. Acad. Sci. U.S.A.* **2003**, *100*, 98.
7. Ferreira, K. N.; Iverson, T. M.; Maghlaoui, K.; Barber, J.; Iwata, S. *Science* **2004**, *303*, 1831.
8. Loll, B.; Kern, J.; Saenger, W.; Zouni, A.; Biesiadka, J. *Nature* **2005**, *438*, 1040.
9. Limburg, J.; Vrettos, J. S.; Liable-Sands, L. M.; Rheingold, A. L.; Crabtree, R. H.; Brudvig, G. W. *Science* **1999**, *283*, 1524.
10. Rüttinger, W.; Yagi, M.; Wolf, K.; Bernasek, S.; Dismukes, G. C. *J. Am. Chem. Soc.* **2000**, *122*, 10353.
11. Limburg, J.; Vrettos, J. S.; Chen, H. Y.; de Paula, J. C.; Crabtree, R. H.; Brudvig, G. W. *J. Am. Chem. Soc.* **2001**, *123*, 423.
12. Schmitt, H.; Lomoth, R.; Magnuson, A.; Park, J.; Fryxelius, J.; Kritikos, M.; Mårtensson, J.; Hammarström, L.; Sun, L.; Åkermark, B. *Chem.—Eur. J.* **2002**, *8*, 3757.
13. Lomoth, R.; Huang, P.; Zheng, J.; Sun, L.; Hammarström, L.; Åkermark, B.; Styring, S. *Eur. J. Inorg. Chem.* **2002**, 2965.
14. Huang, P.; Magnuson, A.; Lomoth, R.; Abrahamsson, M.; Tamm, M.; Sun, L.; van Rotterdam, B.; Park, J.; Hammarström, L.; Åkermark, B.; Styring, S. *J. Inorg. Biochem.* **2002**, *91*, 159.
15. Berg, K. E.; Tran, A.; Raymond, M. K.; Abrahamsson, M.; Wolny, J.; Redon, S.; Andersson, M.; Sun, L.; Styring, S.; Hammarström, L.; Toftlund, H.; Åkermark, B. *Eur. J. Inorg. Chem.* **2001**, 1019.
16. Miller, C. G.; Gordon-Wylie, S. W.; Horwitz, C. P.; Strazisar, S. A.; Periano, D. K.; Clark, G. R.; Weintraub, S. T.; Collins, T. J. *J. Am. Chem. Soc.* **1998**, *120*, 11540.
17. Naruta, Y.; Sasayama, M.; Sasaki, T. *Angew. Chem., Int. Ed. Engl.* **1994**, *33*, 1839.
18. Shimazaki, Y.; Nagano, T.; Takesue, H.; Ye, B.; Tani, F.; Naruta, Y. *Angew. Chem., Int. Ed.* **2004**, *43*, 98.
19. Groves, J. T.; Lee, J.; Marla, S. S. *J. Am. Chem. Soc.* **1997**, *119*, 6269.
20. Jin, N.; Groves, J. T. *J. Am. Chem. Soc.* **1999**, *121*, 2923.
21. Jin, N.; Bourassa, J. L.; Tizio, S. C.; Groves, J. T. *Angew. Chem., Int. Ed.* **2000**, *39*, 3849.
22. Liu, H.-Y.; Lai, T.-S.; Yeung, L.-L.; Chang, C. K. *Org. Lett.* **2003**, *5*, 617.
23. Gross, Z.; Golubkov, G.; Simkhovich, L. *Angew. Chem., Int. Ed.* **2000**, *39*, 4045.
24. Mandimutsira, B. S.; Ramdhanie, B.; Todd, R. C.; Wang, H. L.; Zareba, A. A.; Czernuszewicz, R. S.; Goldberg, D. P. *J. Am. Chem. Soc.* **2002**, *124*, 15170.
25. Meier-Callahan, A. E.; Gray, H. B.; Gross, Z. *Inorg. Chem.* **2000**, *39*, 3605.
26. Vogel, E.; Will, S.; Tilling, A. S.; Neumann, L.; Lex, J.; Bill, E.; Trautwein, A. X.; Wieghart, K. *Angew. Chem., Int. Ed. Engl.* **1994**, *33*, 731.
27. Will, S.; Lex, J.; Vogel, E.; Adamian, V. A.; Van Caemelbecke, E.; Kadish, K. M. *Inorg. Chem.* **1996**, *35*, 5577.
28. Will, S.; Lex, J.; Vogel, E.; Schmickler, H.; Gisselbrecht, J.-P.; Haubtmann, C.; Bernard, M.; Gross, M. *Angew. Chem., Int. Ed.* **1997**, *36*, 357.
29. Golubkov, G.; Bendix, J.; Gray, H. B.; Mahammed, A.; Goldberg, I.; DiBilio, A. J.; Gross, Z. *Angew. Chem., Int. Ed.* **2001**, *40*, 2132.
30. Jérôme, F.; Gros, C. P.; Tardieux, C.; Barbe, J.-M.; Guilard, R. *Chem. Commun.* **1998**, 2007.
31. Guilard, R.; Gros, C. P.; Bolze, F.; Jérôme, F.; Ou, Z.; Shao, J.; Fischer, J.; Weiss, R.; Kadish, K. M. *Inorg. Chem.* **2001**, *40*, 4845.
32. Guilard, R.; Jérôme, F.; Barbe, J.-M.; Gros, C. P.; Ou, Z.; Shao, J.; Fischer, J.; Weiss, R.; Kadish, K. M. *Inorg. Chem.* **2001**, *40*, 4856.
33. Kadish, K. M.; Ou, Z.; Shao, J.; Gros, C. P.; Barbe, J.-M.; Jérôme, F.; Bolze, F.; Burdet, F.; Guilard, R. *Inorg. Chem.* **2002**, *41*, 3990.
34. Kadish, K. M.; Shao, J.; Ou, Z.; Gros, C. P.; Bolze, F.; Barbe, J.-M.; Guilard, R. *Inorg. Chem.* **2003**, *42*, 4062.
35. Guilard, R.; Gros, C. P.; Barbe, J.-M.; Espinosa, E.; Jérôme, F.; Tabard, A.; Latour, J.-M.; Shao, J.; Ou, Z.; Kadish, K. M. *Inorg. Chem.* **2004**, *43*, 7441.
36. Yeh, C.; Chang, C. J.; Nocera, D. G. *J. Am. Chem. Soc.* **2001**, *123*, 1513.
37. Chang, C. J.; Yeh, C.; Nocera, D. G. *J. Org. Chem.* **2002**, *67*, 1403.
38. Gryko, D. T.; Jadach, K. *J. Org. Chem.* **2001**, *66*, 4267.
39. Paolesse, R.; Marini, A.; Nardis, S.; Frollo, A.; Mandoj, F.; Nurco, D. J.; Prodi, L.; Montaltl, M.; Smith, K. M. *J. Porphyrins Phthalocyanines* **2003**, *7*, 25.
40. Steene, E.; Wondimagegn, T.; Ghosh, A. *J. Phys. Chem. B.* **2001**, *105*, 11406.
41. Steene, E.; Wondimagegn, T.; Ghosh, A. *J. Inorg. Biochem.* **2002**, *88*, 113.
42. Gross, Z. *J. Biol. Inorg. Chem.* **2001**, *6*, 733.